ACS APPLIED MATERIALS & INTERFACES

Research Article

www.acsami.org

A Scalable Method toward Superhydrophilic and Underwater Superoleophobic PVDF Membranes for Effective Oil/Water Emulsion Separation

Tao Yuan, Jianqiang Meng,* Tingyu Hao, Zihong Wang, and Yufeng Zhang

State Key Laboratory of Separation Membranes and Membrane Processes, Tianjin Polytechnic University, Tianjin 300387, PR China

Supporting Information

ABSTRACT: A superhydrophilic and underwater superoleophobic PVDF membrane (PVDFAH) has been prepared by surface-coating of a hydrogel onto the membrane surface, and its superior performance for oil/water emulsion separation has been demonstrated. The coated hydrogel was constructed by an interfacial polymerization based on the thiol-epoxy reaction of pentaerythritol tetrakis (3-mercaptopropionate) (PETMP) with diethylene glycol diglycidyl ether (PEGDGE) and simultaneously tethered on an alkaline-treated commercial PVDF membrane surface via the thio-ene reaction. The PVDFAH membranes can be fabricated in a few minutes under mild conditions and show superhydrophilic and underwater superoleophobic properties for a series of organic solvents. Energy dispersive X-ray (EDX) analysis shows that the hydrogel coating was efficient throughout the pore lumen. The membrane shows superior oil/water emulsion separation performance, including high water permeation, quantitative oil rejection, and robust antifouling performance in a series oil/water emulsions, including that prepared from crude oil. In addition, a 24 h Soxhlet-extraction experiment with ethanol/water solution (50:50, v/v) was conducted to test the tethered hydrogel stability. We see that the membrane maintained the water contact angle below 5°, indicating the covalent tethering stability. This technique shows great promise for scalable fabrication of membrane materials for handling practical oil emulsion purification.

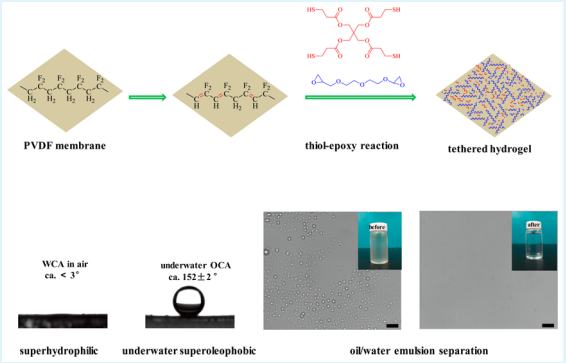

KEYWORDS: *PVDF membrane, surface modification, superhydrophilic, underwater superoleophobic, oil/water separation*

1. INTRODUCTION

Oil/water separation has been in the spotlight worldwide in recent years because of increased production of industrial oily wastewater and increasing environmental awareness.[1−3] From the estimates by OTM & Douglas-Westwood, 241 million barrels of produced water associated with oil and gas operations are globally generated every day, and by 2020, their generation is expected to grow to 292 million barrels.[4] However, oil/water separation remains a technical challenge because of the complex composition and the high oil content of oily wastewater. Traditional remediation methods suffer from low efficiency, high cost as well as second pollution.[5,6] Very recently, membrane filtration has shown great promise as a clean and efficient technology for oily wastewater treatment because of its many advantages, such as high oil-removal efficiency, low energy cost, small footprint, compact design, minimal chemical addition, and others. However, as a novel technology, membrane filtration is still far from being optimized for oil/water emulsion treatment. The biggest challenge is still that of membrane fouling because of surfactant adsorption and pore plugging by oil droplets.[7−9]

Novel membrane materials with superwetting properties have recently evoked a lot of interest for oil/water separation.[10−13] Jiang and co-workers first developed superhydrophobic and superoleophilic coating mesh films for oil/water separation.[14] Since then, there has been continuing interest in the development of membrane filter materials with superwetting properties, either hydrophobic−oleophilic "oil-removing" or hydrophilic−oleophobic "water-removing" properties, for oil/water mixture separation. Typical examples include pH-controllable copper mesh film for oil/water separation,[15,16] superwetting PVDF and its copolymer membranes via specially tailored phase-inversion conditions,[7] a fluorodecyl POSS + *x*-PEGDA blend-coated hygroresponsive mesh membrane,[17] TiO_2 films spray-coated with nanoparticles,[18] and electrospun nanofibrous membranes.[19] These membrane materials usually have a multiscale hierarchical surface structure and show excellent oil/water separation performance, including ultrahigh permeation flux, quantitative oil rejection, and sustainable cycled use. However, the preparation of these materials usually involves carefully tailored nanofabrication methods, which can be very challenging for

Received: April 26, 2015
Accepted: June 24, 2015
Published: June 24, 2015

DOI: 10.1021/acsami.5b03625
ACS Appl. Mater. Interfaces 2015, 7, 14896−14904

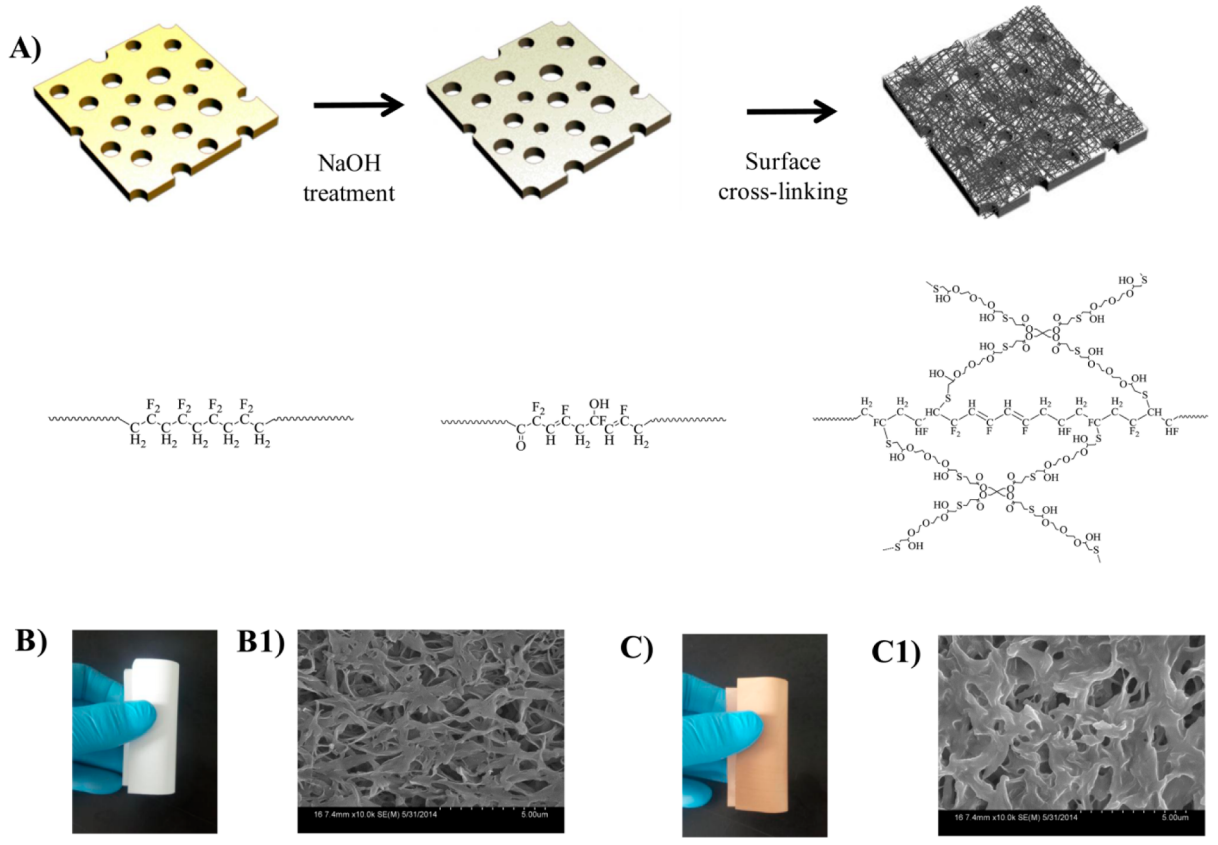

Figure 1. (A) Scheme of the fabrication of PVDFAH membrane. (B) Photograph of PVDF membrane. (B1) SEM image of PVDF membrane. (C) Photograph of PVDFAH membrane. (C1) SEM image of PVDFAH membrane.

large-scale membrane fabrication. In addition, their performance usually was evaluated by dead-end filtration of simulated oil/water mixtures. In contrast, cross-flow filtration is a more widely used operation, and industrial oily wastewater can have a very complex composition. The intense turbulent flow in tube pass and corrosive components in the oily wastewater can be very challenging to the membranes introduced above, especially as far as the mechanical strength and surface chemical stability are concerned.[20−23] In fact, there have been very few works reporting the fouling and rinsing test of the membrane material via long-term cross-flow filtration experiments. Efforts have thus far focused on exploring a robust and scalable technology toward superwetting membranes addressing the need for various oil/water emulsion separations on an industrial scale.

Surface modification of commercial membranes no doubt is the most promising for fabrication of superwetting membranes on a large scale. In recent years, many membrane materials have been endowed with hydrophilic properties by blending with amphiphilic copolymers,[24,25] surface grafting,[26−28] and surface coating.[29−31] Among diverse surface modification technologies, surface coating is the most convenient method and is ready to be fitted into a membrane-coating and rolling line. However, successful application of surface coating in commercial membrane production is still limited, and the major challenges are high cost of the materials, slow reaction process, inevitable flux decline, and degradation of the coating layer in long-term use. To address these challenges toward scalable fabrication of superwetting membranes for oil/water separation, we envisage constructing a permanent and tethered hydrophilic layer on the membrane surface using a rapid and simple reaction with commercial reagents.

Herein, we report the fabrication of a superhydrophilic and underwater superoleophobic polyvinylidene fluoride membrane (PVDFAH) with a cross-linked hydrogel PETMPEG tethered onto the membrane surface (Figure 1). The hydrogel was constructed by interfacial polymerization based on the thiol-epoxy ring-opening reaction between pentaerythritol tetrakis (3-mercaptopropionate) (PETMP) and diethylene glycol diglycidyl ether (PEGDGE). A commercial PVDF membrane was selected as the base membrane because it is a classical membrane for water treatment with excellent mechanical and thermal stability as well as high chemical resistance, except under strong alkaline conditions, in which case C═C bonds can be introduced onto PVDF membrane surface as anchors to tether hydrogels via the thio-ene reaction. The thiol-epoxy ring-opening reaction was selected because of its high reaction efficiency, quantitative conversion, and ultrafast reaction kinetics, which are characteristic of "click" chemistry.[32−34] The hydrogel formation was found to be instantaneous (details in the Supporting Information, Figure S1), and the coating can be accomplished in several minutes. Surface physio-chemical properties, oil/water emulsion filtration performance, antifouling performance and durability of the tethered hydrogel were investigated in detail.

2. EXPERIMENTAL SECTION

2.1. Materials and Reagents. The PVDF membrane used was purchased from Millipore, Ltd. (Immobilon-P, 0.22 μm). Pentaerythritol tetrakis (3-mercaptopropionate) (PETMP), diethylene glycol diglycidyl ether (PEGDGE), and tetrabutylammonium fluoride trihydrate (TBAF) were supplied by Aldrich, Co. All the other chemicals were used as received unless otherwise noted.

DOI: 10.1021/acsami.5b03625
ACS Appl. Mater. Interfaces 2015, 7, 14896−14904

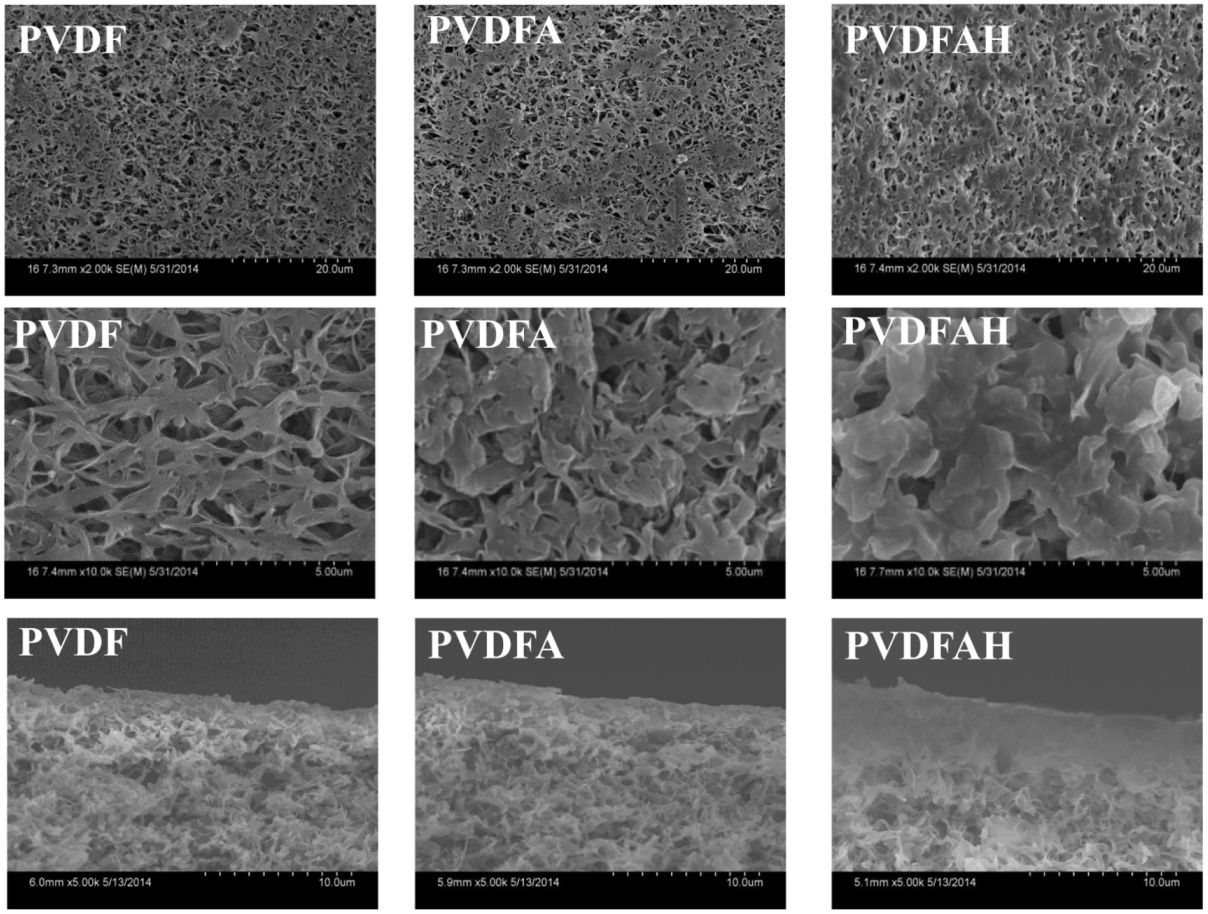

Figure 2. SEM images of membrane surface (top, 2000×; middle, 10 000×; and bottom, cross-sectional view). Columns show from left to right, respectively, PVDF membrane, PVDFA membrane, and PVDFAH membrane.

2.2. Fabrication of the PVDFAH Membrane. The PVDFAH membrane was fabricated by an interfacial polymerization based on the thiol-epoxy ring-opening reaction between PETMP and PEGDGE on an alkaline-treated PVDF membrane (PVDFA). Initially, the PVDF membrane was treated with a 1.25 M NaOH/ethanol solution at 80 °C for 30 s and rinsed with ethanol. The membrane was then immersed in a 0.07 M PETMP/AIBN (6:1, moL/moL) in acetone solution and kept under shaking for 2 min. After evaporating acetone for 1 min, the membrane was immersed into a 0.15 M PEGDGE/TBAF (7:1, moL/moL) ethanol solution for another 2 min. After that, the membrane was heated at 90 °C for 5 min. The obtained PVDFAH membrane was rinsed with ethanol, acetone, and water in turn and dried at 50 °C for 2 h.

2.3. Oily Emulsion Samples Preparation. In this work, a series of surfactant-stabilized oil-in-water emulsions, including an SDS/gasoline/H_2O emulsion, an SDS/*n*-dodecane/H_2O emulsion, an SDS/*n*-hexadecane/H_2O emulsion, and an SDS/crude oil/H_2O emulsion were prepared in-house by mixing 1.5 g of oil, 200 mg of SDS, and 1 L of DI water with the aid of sonification for 30 min.

2.4. Oil/Water Emulsion Filtration Experiments. To evaluate the oil/water separation, water permeation, and antifouling performance, the cross-flow filtration operation was performed with six serial connection cells for flat membranes at 25 °C (details in the Supporting Information, Figure S2). Initially, the pure water permeation (J_{w0}) was recorded at 0.02 MPa after it became steady at 0.1 MPa, and then the oily emulsion was introduced. The evolution of water permeation was recorded over the whole process of oily emulsion filtration at 0.02 MPa, and the filtrate was withdrawn for total organic carbon analysis (TOC). Finally, the membrane was washed with DI water for 2−3 min, and then, the pure water permeation (J_{wi}) was recorded. The pure water permeation was calculated via eq 1:

$$J = \frac{V}{A\Delta tP} \tag{1}$$

and the flux recovery (FR) was calculated via eq 2:

$$\mathrm{FR} = \frac{J_{wi}}{J_{w0}} \times 100\% \tag{2}$$

where J is the water permeation of membrane (L m^{-2} h^{-2} bar^{-1}), V is the volume of the permeate (L), A is the effective area of membrane (m^2), Δt represents the testing time (h), and P is the operating pressure (bar).

2.5. Instruments and Measurements. The observation of membrane surface morphology and EDX analysis were conducted on a field-emission scanning electron microscopy system (FESEM, Hitachi S-4800, Japan). FTIR spectra were recorded using a Vector-22 spectrometer (Bruker Daltonic Inc., Germany). The Raman spectra were observed with a Thermo Scientific DXR Raman microscope using a green laser with wavelength at 532 nm and power level at 1.0 mW over a range of 600−2400 cm^{-1} for all of the membrane samples. XPS measurements were conducted on a Quanta 200 spectrometer (FEI Co., Ltd. USA). The contact angle (CA) values were obtained by measuring more than five different positions of the same sample at 25 °C using the sessile drop method on a contact angle meter (Drop Shape Analysis100, KRUSS BmbH Co., Germany). The underwater oil adhesion forces were measured by a high-sensitivity micro-electromechanical balance system (Data-Physics, DCAT11, Germany). The adhesion forces were recorded when an oil droplet (2 μL) was suspended with a metal cap and controlled to contact with the surface of the PVDFAH membrane at a constant speed of 0.005 mm s^{-1} and then to leave. Droplet size distributions of the oily emulsion samples were analyzed by a LA-300 laser-scattering particle size distribution

DOI: 10.1021/acsami.5b03625
ACS Appl. Mater. Interfaces 2015, 7, 14896−14904

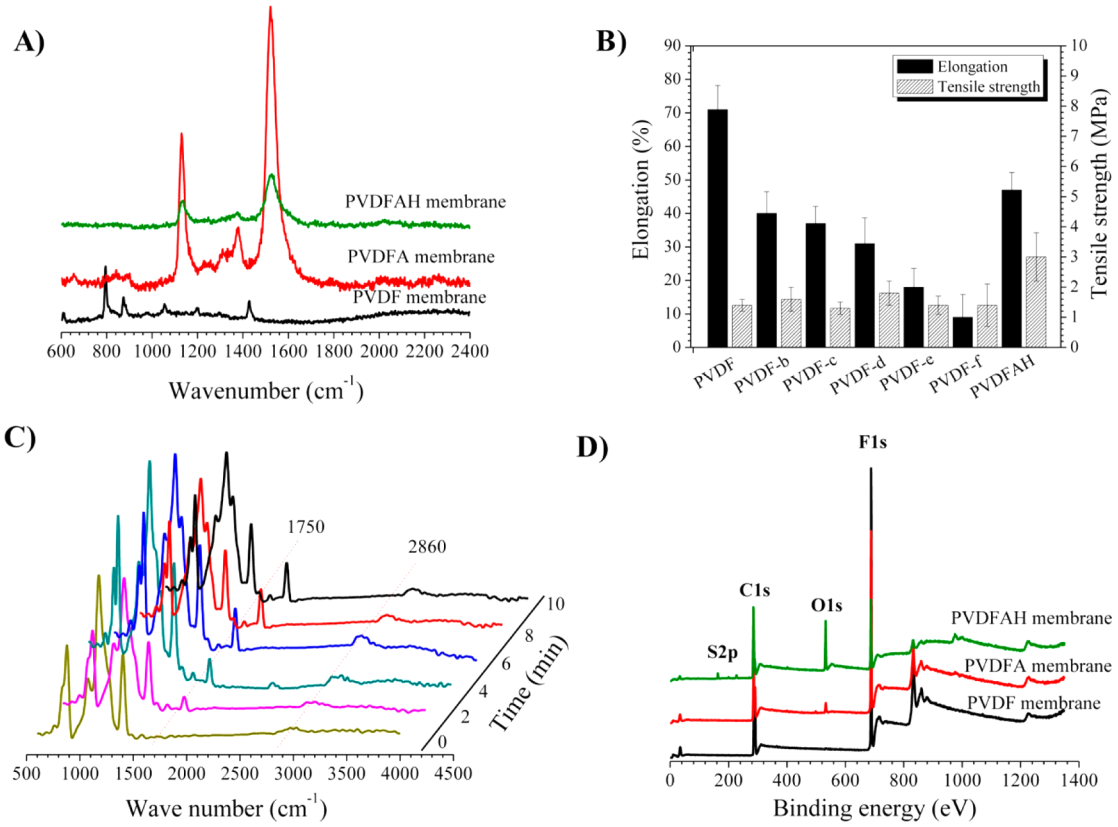

Figure 3. (A) Raman spectra of the membrane surface. (B) Elongation and tensile strength of the PVDFA membranes via alkaline treatment for 30 s (PVDF-b), alkaline treatment for 60 s (PVDF-c), alkaline treatment for 120 s (PVDF-d), alkaline treatment for 180 s (PVDF-e), alkaline treatment for 300 s (PVDF-f), and the PVDFAH membrane. (C) FTIR spectra of the fabricated PVDFAH membrane with different heat treatment times at 90 °C. (D) XPS wide-scan spectra of the membranes.

analyzer (Horiba Stec, Co., Ltd., Japan). A total organic carbon analyzer ET1020A (Euro Tech Ltd., UK) was used for oil concentration analysis. The optical microscopy images of the oily emulsion samples were observed by a BX51-P polarizing microscope (Olympus Optical Co., Ltd., Japan).

3. RESULTS AND DISCUSSION

3.1. Membrane Morphology. A number of studies have illustrated that a high surface roughness contributes greatly to membrane superhydrophilicity.[35−38] The surface and cross-sectional morphologies of the PVDF, PVDFA, and PVDFAH membranes are shown in Figure 2. Compared with the PVDF membrane, the PVDFAH membrane has a rather rougher and denser surface morphology as well as thicker pore walls. A dense hydrogel coating on the PVDFAH membrane can also be observed from the cross-sectional images. The enhanced surface roughness caused by the PETMPEG hydrogel layer would contribute to more water molecules being trapped or gathering onto the membrane surface.[39]

3.2. Chemical Constitution of the Membrane Surface. The PVDF membrane was treated with alkaline solution to produce ethylene groups for PETMPEG hydrogel anchoring. Raman spectroscopy was used for surface analysis because of its unique ability to estimate the content of conjugation C═C bonds on the PVDFA membrane surface.[40,41] As shown in Figure 3A, the peaks at 1129 and 1525 cm^{-1} are representative of C−C and C═C respectively. We see their intensities for PVDFA membrane are much greater than those for PVDF membrane, indicating the formation of conjugated carbon double bonds during the alkaline treatment. Note that the intensity of the C═C bond on the PVDFAH membrane decreased obviously after hydrogel coating. This result illustrates that the thiol-ene addition reaction occurred simultaneously with the thiol-epoxy reaction.

Alkaline treatment can deteriorate the mechanical strength of PVDF membrane by eliminating HF. The effect of alkaline treatment on membrane mechanical strength was investigated in detail to select a condition under which a sufficient amount of C═C bonds were introduced without significant deterioration of the mechanical strength. The results are shown in Figure 3B. It should be noted that a proper alkaline treatment condition can vary for different PVDF membranes. Many reports introduced much harsher conditions for the efficient formation of C═C bonds.[40,41] This phenomenon can be related to different crystallinities of PVDF membranes caused by different membrane processing methods. A 1.25 mol/L NaOH/ethanol solution was used to introduce C═C bonds onto the PVDF membrane surface. Finally, the PVDF membrane was treated for 30 s. The obtained PVDFA membrane has a tensile strength of 1.6 MPa and elongation of 48%, which is sufficient for a typical UF/MF operation. It is interesting to see that the tensile strength of the membrane was significantly enhanced after surface tethering of the PETMPEG hydrogel. Finally, the tensile strength of the PVDFAH membrane is about twice that of the pristine PVDF membrane. This result is believed to be due to the incorporation of the highly cross-linked thiol-epoxy networks. The doubled tensile strength of the PVDFAH membrane compared to that of

DOI: 10.1021/acsami.5b03625
ACS Appl. Mater. Interfaces 2015, 7, 14896−14904

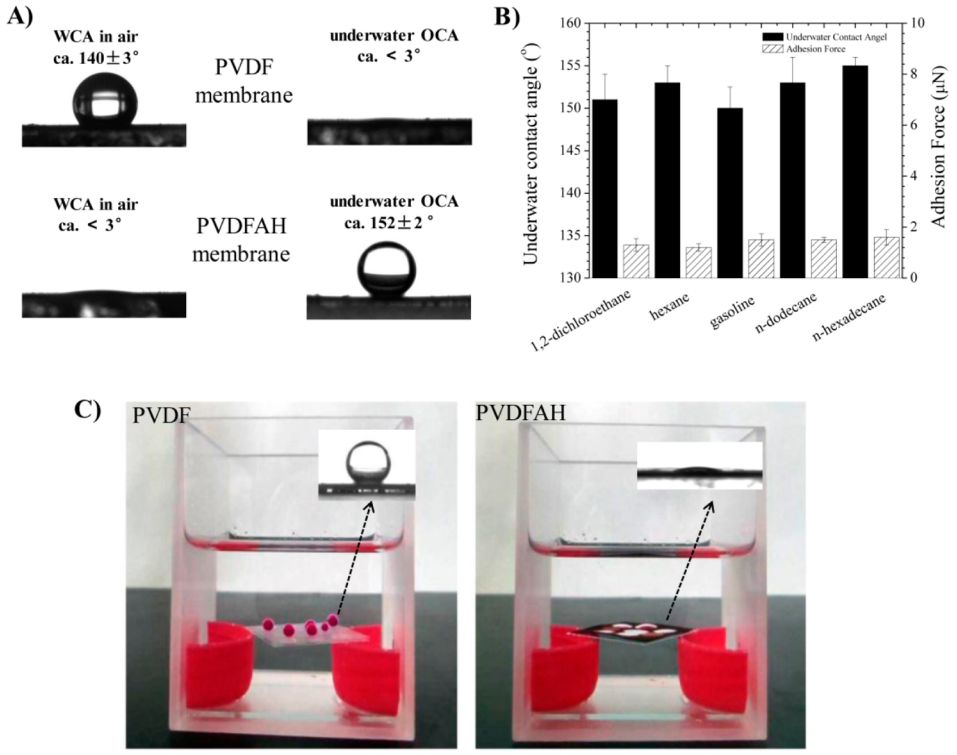

Figure 4. (A) WCAs in air and underwater OCAs of PVDF membrane and PVDFAH membrane. (B) Underwater OCAs and underwater adhesion forces of PVDFAH membranes for series oils. (C) Water wetting phenomena of PVDF and PVDFAH membrane under *n*-dodecane.

PVDF membrane ensures its application in harsh oil−wastewater filtration applications.

Figure 3C shows the FTIR spectra of the PVDFAH membranes fabricated with different heat treatment times at 90 °C. It can be seen that the vibrational peak intensity of C═O, $-CH_2$, and −OH groups at 1750, 2890, and 3400 cm^{-1}, respectively, increased obviously at the beginning and tended to stabilize after 4 min of heat treatment indicating successful and rapid coating of the PETMPEG hydrogel on the membrane surface. A uniform coating over the whole membrane surface ensures complete shielding of the hydrophobic substrate underneath and thus robust antifouling performance. However, surface coating on the pore wall remains a challenge for membrane chemists because of the hindered diffusion of the reactants. The constituent elements of the membrane surface were probed by XPS. Figure 3D shows that O element increased obviously on the PVDFAH membrane upon introducing the hydrogel. The adding of O element is believed to play an important role in improving the membrane hydrophilic property.[42−44] The C 1s core-level spectra (Supporting Information, Figure S3) show the decrease of CF_2-CH_2 adsorption and the booming of $C(O)-CH_2$ and CH_2-O-CH_2 adsorption, which confirmed successful tethering of the PETMPEG hydrogel. The CH_2-O-CH_2 adsorption shows the highest intensity among the splitted peaks, which corresponds to the coverage of the hydrogel on the membrane surface. Note here that the presence of the conjugated structures cannot be detected by XPS because the adsorptions of $(-CH=CH-)_n$ and $(-CH_2-CH_2-)_n$ overlap. In addition, the O element content of PVDFAH membrane booms to 17% after tethering PETMPEG hydrogel, yet PVDF has no O element detection, indicating sufficient hydrogel coverage on membrane top surface (details in the Supporting Information, Table S1).

EDX analysis helps to characterize the hydrogel distribution on the pore wall throughout the pore lumen (details in the Supporting Information, Table S2). Several spots on the membrane cross section from the top surface to the bottom surface were selected for observation. We see that the O element content of the inner pore wall is still fairly high (5.9%), although it decreases from 9.9% at the top surface and then recovers to 7.1% at the bottom surface. This result indicates sufficient surface coating on the pore wall of the inner layer. This phenomenon should benefit from a highly efficient reaction of small molecules on a large-pore-size membrane.

3.3. Membrane Wettability. The surface-wetting properties of the membranes were studied by water contact angle (WCA) measurements. The PVDFAH membrane shows a WCA below 3° in air (completely wetted in 5 s) and an underwater oil contact angle (OCA) of 152 ± 2° for *n*-dodecane (Figure 4A), thus demonstrating typical superhydrophilic and underwater superoleophobic properties. Underwater OCAs and oil adhesion forces of the PVDFAH membrane were also measured for several organic solvents, including 1,2-dichloroethane, hexane, gasoline, and *n*-hexadecane (Figure 4B). All of the OCAs are greater than 150°, confirming the underwater superoleophobic properties of the PVDFAH membrane. In contrast, the PVDF membrane has a WCA of 140 ± 3° in air and OCA of less than 3° underwater. All the oil adhesion force values were below 2 μN (Figure 4B), which is consistent with the membranes reported with superhydrophilic and underwater superoleophobic properties.[14] Water-wetting properties in *n*-dodecane were also observed for PVDF and PVDFAH membrane (Figure 4 C). We see that the water droplet spread quickly after injecting a drop of water on the PVDFAH membrane surface, and its WCA under oil is less than 5°. In contrast, the water droplet was squeezed away from the PVDF membrane surface by the surrounding oil (details in

DOI: 10.1021/acsami.5b03625
ACS Appl. Mater. Interfaces 2015, 7, 14896−14904

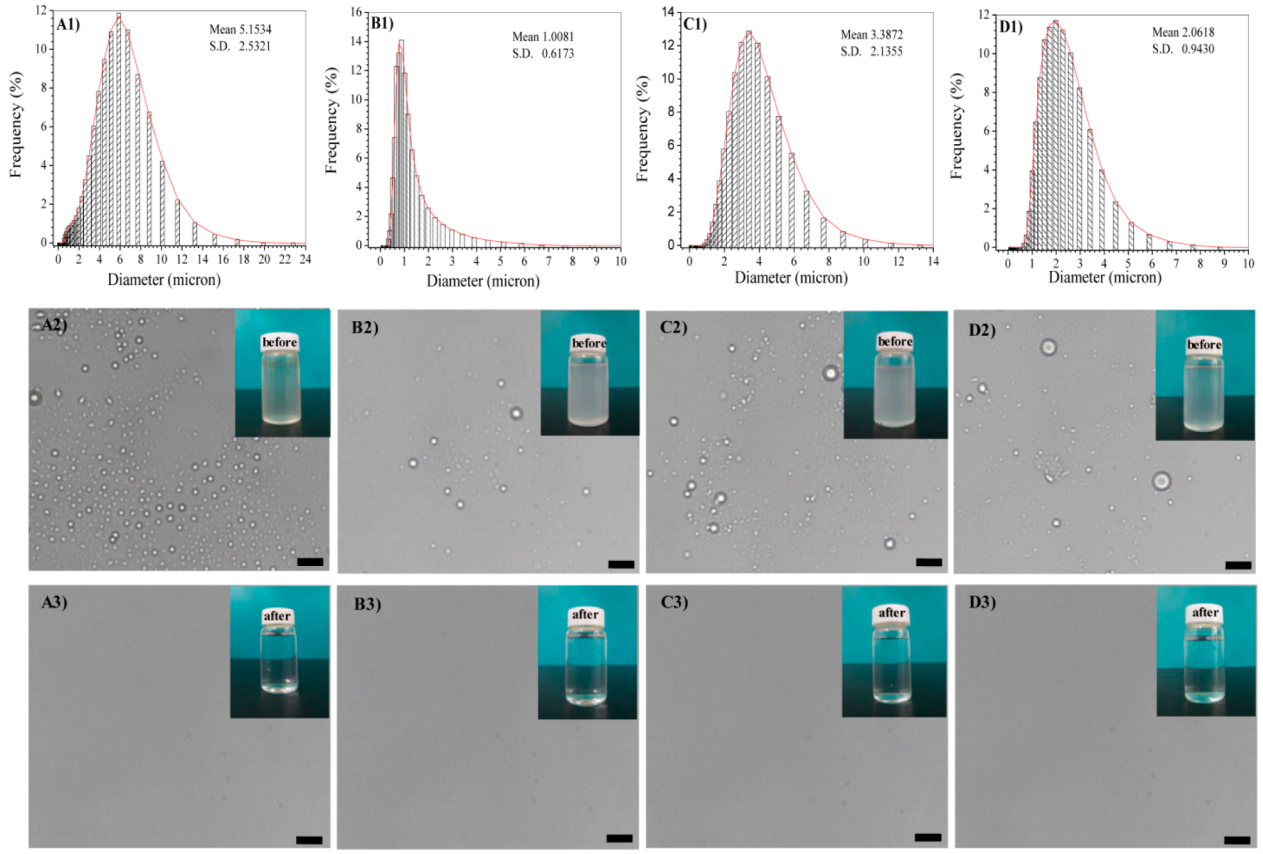

Figure 5. (A1−D1) Droplet size distribution. Optical microscopy images of the emulsions (A2−D2) before and (A3−D3) after filtration. Columns feature A, SDS/gasoline/H_2O emulsion; B, SDS/*n*-dodecane/H_2O emulsion; C, SDS/*n*-hexadecane/H_2O; and D, SDS/crude oil/H_2O. Scale bars = 20 μm.

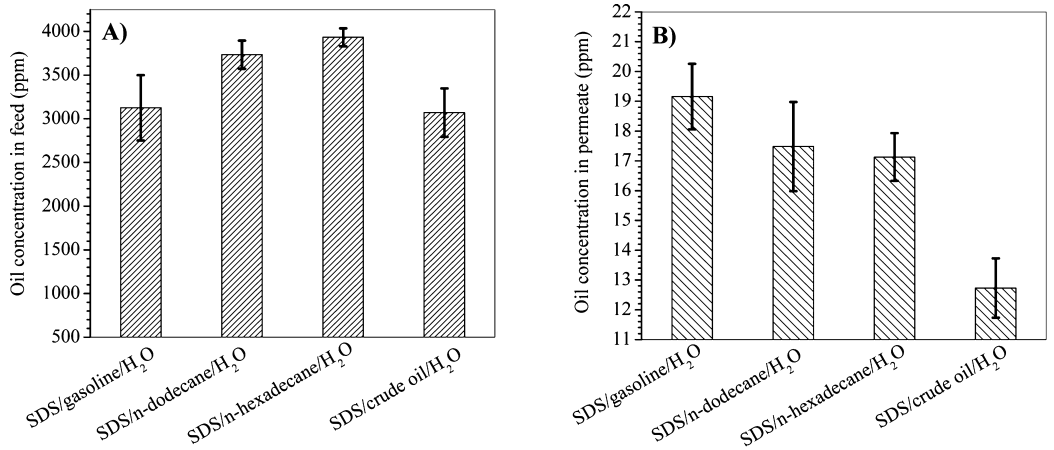

Figure 6. TOC values of the (A) feed and (B) permeate.

the Supporting Information, Figure S4). The different water-wetting properties in *n*-dodecane for the PVDF membrane and PVDFAH membranes are attributed to their different surface-wetting properties. High oil content can be trapped in the microstructures of the PVDF membrane surface, forming a repulsive oil layer and precluding water contact with the surface, which significantly reduce the contact area and lead to high WCA values. As a comparison, the spontaneous spreading of water on the PVDFAH surface in *n*-dodecane is driven by high affinity of the PVDFAH membrane to water molecules.

The surface-wetting properties of water and oil on membrane surfaces were also evaluated by a soaking−elution experiment. After being soaked in *n*-dodecane, the membranes were immersed in water to evaluate the oil adhesion on the membrane surface. Interestingly, the oil film accumulated very quickly into large droplets and floated up to the water surface (Supporting Information Video 1). In contrast, the adhered oil was difficult to remove from the PVDF membrane surface, even by fierce shaking of the membrane (Supporting Information Video 2).

3.4. Oil/Water Emulsion Filtration. To evaluate the separation and antifouling performance of the PVDFAH membrane, a series of surfactant-stabilized oil-in-water emulsions were prepared in-house. It can be seen from Figure

DOI: 10.1021/acsami.5b03625
ACS Appl. Mater. Interfaces 2015, 7, 14896−14904

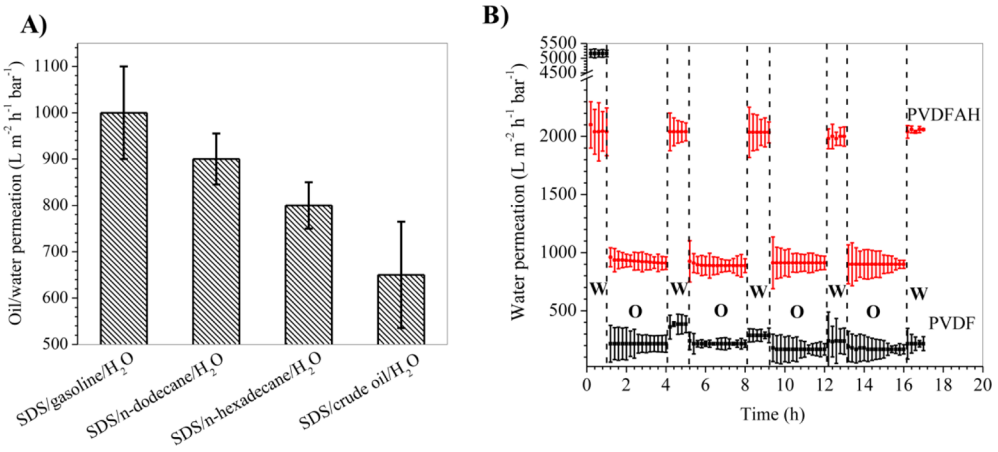

Figure 7. (A) Oil/water permeation of the PVDFAH membrane for a series of emulsions and (B) water permeation evolutions in an 18 h and 4-cycle water (W) and SDS/*n*-dodecane/H_2O emulsion (O) filtration process.

5 that all of the emulsion samples have wide droplet size distributions. After filtration, the permeate are transparent, and no oil droplets can be seen in optical microscopy images, indicating an effective oil/water separation. It should be noted that the droplet size distribution data of the permeate could not be obtained by the laser-scattering method because of the minimal content of the oil droplets in the permeate.

Figure 6 shows the oil concentration of the feed and permeate as determined by TOC. It can be seen that the oil concentration in permeate was obviously lower than the feed. Note that the TOC values in permeate were still 10−20 mg/L, which may be caused by the dissolved SDS.[7] In spite of the high TOC values in the feed, the oil rejections are still higher than 99%, indicating effective oil/water separation performance of the PVDFAH membrane.

Membrane permeation was observed, as shown in Figure 7A. The PVDFAH membrane showed stable oil/water permeation such as 1000 ± 100 L m^{-2} h^{-1} bar^{-1} for SDS/gasoline/water emulsion, 900 ± 55 L m^{-2} h^{-1} bar^{-1} for SDS/*n*-dodecane/water emulsion, 800 ± 50 L m^{-2} h^{-1} bar^{-1} for SDS/*n*-hexadecane/water emulsion, and 650 ± 115 L m^{-2} h^{-1} bar^{-1} for SDS/crude oil/water emulsion. These values are several times higher than those of traditional filtration membranes.[45,46] The flux variation for different emulsions should be due to the viscosity difference.[18,19]

As for an oil emulsion filtration membrane, antifouling performance is more important than permeation and rejection themselves. As Figure 7B shows, an 18 h and 4-cycle filtration was performed using the SDS/*n*-dodecane/water emulsion as the feed. The membrane was simply rinsed by a 2 min water washing following each emulsion filtration operation. It can be seen that the PVDFAH membrane almost completely recovers its initial flux after each rinsing and still keeps a stable pure-water permeation of 2000 L m^{-2} h^{-1} bar^{-1} and an emulsion flux of 900 L m^{-2} h^{-1} bar^{-1} after the 18 h test. In contrast, a continuous flux decline was observed for PVDF membrane, which has a final emulsion flux of 168 L m^{-2} h^{-1} bar^{-1}. Robust antifouling performance is believed to be important for practical applications.

3.5. PETMPEG Hydrogel Stability. The long-term durability of the coated hydrogel was evaluated by a 24 h Soxhlet-extraction experiment using ethanol/water (1:1, v/v) solution. The WCA results as a function of the extraction time were shown in Figure 8. The membrane directly coated with

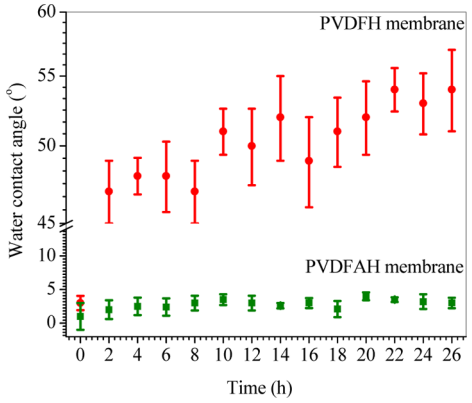

Figure 8. Evolution of the WCA values of PVDFH and PVDFAH membranes in a 24 h Soxhlet-extraction experiment.

PETMPEG hydrogel (PVDFH membrane) was used as a control. Obviously, the PVDFAH membrane maintains its WCA below 5°, whereas the PVDFH membrane gradually loses its surface hydrophilicity. The robustness of the PVDFAH membrane performance is believed to be contributed by the covalent tethering of the hydrogel.

4. CONCLUSIONS

A hydrogel-tethered PVDF membrane with superhydrophilic and underwater superoleophobic properties has been developed for effective oil/water emulsion separation. The membrane was prepared by a rapid and facile surface modification process based on a commercial membrane. In addition to high water permeation flux and quantitative oil rejection, the obtained membranes show superior mechanical properties and antifouling performance in a series of oil/water emulsion filtration tests. Together with the robustness of the tethered hydrogel layer, the reported method shows great promise for scalable fabrication of membrane materials for handling practical oil emulsion purification.

■ ASSOCIATED CONTENT

Supporting Information

Rapid formation of the free-standing PETMPEG hydrogel, the cross-flow filtration testing equipment, mechanical properties of the membranes, the XPS C 1s core-level spectra for the membranes, water droplet wetting properties on membrane

DOI: 10.1021/acsami.5b03625
ACS Appl. Mater. Interfaces 2015, 7, 14896−14904

surface under *n*-dodecane, chemical compositions of the membrane surface by XPS, chemical composition distribution of PVDFAH membrane pore lumen by EDX, soaking−elution experiment videos (Videos 1 and 2). The Supporting Information is available free of charge on the ACS Publications website at DOI: 10.1021/acsami.5b03625.

AUTHOR INFORMATION

Corresponding Author

*E-mail: jianqiang.meng@hotmail.com. Phone: +86 22 83955078. Fax: +86 22 83955055.

Notes

The authors declare no competing financial interest.

ACKNOWLEDGMENTS

We gratefully acknowledge support from the National Natural Science Foundation of China (grant no. 21274108) and the Program for Chang-jiang Scholars and Innovative Research Team in University of Ministry of Education of China (grant no. IRT13084).

REFERENCES

(1) Zhu, Y. Z.; Wang, D.; Jiang, L.; Jin, J. Recent Progress in Developing Advanced Membranes for Emulsified Oil/Water Separation. *NPG Asia Mater.* **2014**, *6*, e101.

(2) Sagle, A. C.; Ju, H.; Freeman, B. D.; Sharma, M. M. PEG-Based Hydrogel Membrane Coatings. *Polymer* **2009**, *50*, 756−766.

(3) Liu, N.; Cao, Y. Z.; Lin, X.; Chen, Y. N.; Feng, L.; Wei, Y. A Facile Solvent-Manipulated Mesh for Reversible Oil/Water Separation. *ACS Appl. Mater. Interfaces* **2014**, *6*, 12821−12826.

(4) OTM Consulting & Douglas-Westwood. *World Onshore Produced Water Gamechanger Market Report 2012−2020*; Douglas-Westwood: Houston, TX.

(5) Cheryan, M.; Rajagopalan, N. Membrane Processing of Oily Streams. Wastewater Treatment and waste reduction. *J. Membr. Sci.* **1998**, *151*, 13−28.

(6) Križan Milić, J.; Muric, A.; Petrinic, I.; Simonic, M. Recent Developments in Membrane Treatment of Spent Cutting-Oils: A Review. *Ind. Eng. Chem. Res.* **2013**, *52*, 7603−7616.

(7) Zhang, W. B.; Zhu, Y. Z.; Liu, X.; Wang, D.; Li, J. Y.; Jiang, L.; Jin, J. Salt-Induced Fabrication of Superhydrophilic and Underwater Superoleophobic PAA-g-PVDF Membranes for Effective Separation of Oil-in-Water Emulsions. *Angew. Chem., Int. Ed.* **2014**, *53*, 856−860.

(8) Kasemset, S.; Lee, A.; Miller, D. J.; Freeman, B. D.; Sharma, M. M. Effect of Polydopamine Deposition Conditions on Fouling Resistance, Physical Properties, and Permeation Properties of Reverse Osmosis Membranes in Oil/Water Separation. *J. Membr. Sci.* **2013**, *425-426*, 208−216.

(9) Kim, D. G.; Kang, H.; Han, S.; Lee, J. C. Dual Effective Organic/Inorganic Hybrid Star-Shaped Polymer Coatings on Ultrafiltration Membrane for Bio- and Oil-Fouling Resistance. *ACS Appl. Mater. Interfaces* **2012**, *4*, 5898−5906.

(10) Xue, Z. X.; Jiang, L. Bioinspired Underwater Superoleophobic Surfaces. *Acta Polym. Sin.* **2012**, *10*, 1091−1101.

(11) Zhang, J. P.; Seeger, S. Polyester Materials with Superwetting Silicone Nanofilaments for Oil/Water Separation and Selective Oil Absorption. *Adv. Funct. Mater.* **2011**, *21*, 4699−4704.

(12) Yoon, H.; Na, S. H.; Choi, J. Y.; Latthe, S. S.; Swihart, M. T.; Al-Deyab, S. S.; Yoon, S. S. Gravity-Driven Hybrid Membrane for Oleophobic-Superhydrophilic Oil Water Separation and Water Purification by Graphene. *Langmuir* **2014**, *30*, 11761−11769.

(13) Gao, S. J.; Shi, Z.; Zhang, W. B.; Zhang, F.; Jin, J. Photoinduced Superwetting Single-Walled Carbon Nanotube/TiO2 Ultrathin Network Films for Ultrafast Separation of Oil-in-Water Emulsions. *ACS Nano* **2014**, *8*, 6344−6352.

(14) Feng, L.; Zhang, Z. Y.; Mai, Z. H.; Ma, Y. M.; Liu, B. Q.; Jiang, L.; Zhu, D. B. A Super-Hydrophobic and Super-Oleophilic Coating Mesh Film for the Separation of Oil and Water. *Angew. Chem., Int. Ed.* **2004**, *43*, 2012−2014.

(15) Cheng, Z. J.; Wang, J. W.; Lai, H.; Du, Y.; Hou, R.; Li, C.; Zhang, N. Q.; Sun, K. N. pH-Controllable On-Demand Oil/Water Separation on the Switchable Superhydrophobic/Superhydrophilic and Underwater Low-Adhesive Superoleophobic Copper Mesh Film. *Langmuir* **2015**, *31*, 1393−1399.

(16) Cheng, Z. J.; Lai, H.; Du, Y.; Fu, K. W.; Hou, R.; Li, C.; Zhang, N. Q.; Sun, K. N. pH-Induced Reversible Wetting Transition between the Underwater Superoleophilicity and Superoleophobicity. *ACS Appl. Mater. Interfaces* **2014**, *6*, 636−641.

(17) Kota, A. K.; Kwon, G.; Choi, W.; Mabry, J. M.; Tuteja, A. Hygro-Responsive Membranes for Effective Oil-Water Separation. *Nat. Commun.* **2012**, *3*, 1025−1032.

(18) Gondal, M. A.; Sadullah, M. S.; Dastageer, M. A.; McKinley, G. H.; Panchanathan, D.; Varanasi, K. K. Study of Factors Governing Oil−Water Separation Process Using TiO_2 Films Prepared by Spray Deposition of Nanoparticle Dispersions. *ACS Appl. Mater. Interfaces* **2014**, *6*, 13422−13429.

(19) Tai, M. H.; Gao, P.; Tan, B. Y. L.; Sun, D. D.; Leckie, J. O. Highly Efficient and Flexible Electrospun Carbon-Silica Nanofibrous Membrane for Ultrafast Gravity-Driven Oil-Water Separation. *ACS Appl. Mater. Interfaces* **2014**, *6*, 9393−9401.

(20) Mota, M.; Teixeira, J. A.; Yelshin, A. Influence of Cell-Shape on the Cake Resistance in Dead-End and Cross-Flow Filtrations. *Sep. Purif. Technol.* **2002**, *27*, 137−144.

(21) Becht, N. O.; Malik, D. J.; Tarleton, E. S. Evaluation and Comparison of Protein Ultrafiltration Test Results: Dead-End Stirred Cell Compared with a Cross-Flow System. *Sep. Purif. Technol.* **2008**, *62*, 228−239.

(22) Miller, D. J.; Kasemset, S.; Paul, D. R.; Freeman, B. D. Comparison of Membrane Fouling at Constant Flux and Constant Transmembrane Pressure Conditions. *J. Membr. Sci.* **2014**, *454*, 505−515.

(23) Miller, D. J.; Kasemset, S.; Wang, L.; Paul, D. R.; Freeman, B. D. Constant Flux Crossflow Filtration Evaluation of Surface-modified Fouling-Resistant Membranes. *J. Membr. Sci.* **2014**, *452*, 171−183.

(24) Asatekin, A.; Mayes, A. Oil Industry Wastewater Treatment with Fouling Resistant Membranes Containing Amphiphilic Comb Copolymers. *Environ. Sci. Technol.* **2009**, *43*, 4487−4492.

(25) Zhao, Y. F.; Zhu, L. P.; Yi, Z.; Zhu, B. K.; Xu, Y. Y. Improving the Hydrophilicity and Fouling-Resistance of Polysulfone Ultrafiltration Membranes via Surface Zwitterionicalization Mediated by Polysulfone-Based Triblock Copolymer Additive. *J. Membr. Sci.* **2013**, *440*, 40−47.

(26) Wandera, D.; Himstedt, H. H.; Marroquin, M.; Wickramasinghe, S. R.; Husson, S. M. Modification of Ultrafiltration Membranes with Block Copolymer Nanolayers for Produced Water Treatment: The Roles of Polymer Chain Density and Polymerization Time on Performance. *J. Membr. Sci.* **2012**, *403-404*, 250−260.

(27) Chen, W. J.; Su, Y. L.; Zheng, L. L.; Wang, L. J.; Jiang, Z. Y. The Improved Oil/Water Separation Performance of Cellulose Acetate-Graft-Polyacrylonitrile Membranes. *J. Membr. Sci.* **2009**, *337*, 98−105.

(28) Jing, B. X.; Wang, H. T.; Lin, K. Y.; McGinn, P. J.; Na, C. Z.; Zhu, Y. X. A Facile Method to Functionalize Engineering Solid Membrane Supports for Rapid and Efficient Oil-Water Separation. *Polymer* **2013**, *54*, 5771−5778.

(29) Ju, H.; McCloskey, B. D.; Sagle, A. C.; Wu, Y. H.; Kusuma, V. A.; Freeman, B. D. Crosslinked Poly(ethylene oxide) Fouling Resistant Coating Materials for Oil/Water Separation. *J. Membr. Sci.* **2008**, *307*, 260−267.

(30) Jiang, J. H.; Zhu, L. P.; Zhu, L. J.; Zhang, H. T.; Zhu, B. K.; Xu, Y. Y. Antifouling and Antimicrobial Polymer Membranes based on Bioinspired Polydopamine and Strong Hydrogen-bonded Poly(N-vinyl pyrrolidone). *ACS Appl. Mater. Interfaces* **2013**, *5*, 12895−12904.

DOI: 10.1021/acsami.5b03625
ACS Appl. Mater. Interfaces 2015, 7, 14896−14904

(31) Ejaz Ahmed, F.; Lalia, B. S.; Hilal, N.; Hashaikeh, R. Underwater Superoleophobic Cellulose/Electrospun PVDF−HFP Membranes for Efficient Oil/Water Separation. *Desalination* **2014**, *344*, 48−54.
(32) Mazurek, P.; Daugaard, A. E.; Skolimowski, M.; Hvilsted, S.; Skov, A. L. Preparing Mono-Dispersed Liquid Core PDMS Microcapsules from Thiol-Ene-Epoxy-Tailored Tlow-focusing Microfluidic Devices. *RSC Adv.* **2015**, *5*, 15379−15386.
(33) Cengiz, N.; Rao, J. Y.; Sanyal, A.; Khan, A. Designing Functionalizable Hydrogels Through Thiol-Epoxy Coupling Chemistry. *Chem. Commun.* **2013**, *49*, 11191−11193.
(34) De, S.; Khan, A. Efficient Synthesis of Multifunctional Polymers via Thiol-Epoxy ″Click″ Chemistry. *Chem. Commun.* **2012**, *48*, 3130−3132.
(35) Drelich, J.; Chibowski, E. Superhydrophilic and Superwetting Surfaces: Definition and Mechanisms of Control. *Langmuir* **2010**, *26*, 18621−18623.
(36) Shirtcliffe, N. J.; McHale, G.; Atherton, S.; Newton, M. I. An Introduction to Superhydrophobicity. *Adv. Colloid Interface Sci.* **2010**, *161*, 124−138.
(37) Jung, Y. C.; Bhushan, B. Wetting Behavior of Water and Oil Droplets in Three-Phase Interfaces for Hydrophobicity/philicity and Oleophobicity/philicity. *Langmuir* **2009**, *25*, 14165−14173.
(38) Jin, M. H.; Wang, J.; Yao, X.; Liao, M. Y.; Zhao, Y.; Jiang, L. Underwater Oil Capture by a Three-Dimensional Network Architectured Organosilane Surface. *Adv. Mater.* **2011**, *23*, 2861−2864.
(39) Liu, M. J.; Wang, S. T.; Wei, Z. X.; Song, Y. L.; Jiang, L. Bioinspired Design of a Superoleophobic and Low Adhesive Water/Solid Interface. *Adv. Mater.* **2009**, *21*, 665−669.
(40) Brewis, D. M.; Mathieson, I.; Sutherland, I. Pretreatment of Poly(vinyl fluoride) and Poly(vinylidene fluoride) with Potassium Hydroxide. *Int. J. Adhes. Adhes.* **1996**, *16*, 87−95.
(41) Ross, G. J.; Watts, J. F.; Hill, M. P.; Morrissey, P. Surface Modification of Poly(vinylidene fluoride) by Alkaline Treatment 1. The Degradation Mechanism. *Polymer* **2000**, *41*, 1685−1696.
(42) Guo, H. F.; Ulbricht, M. Surface Modification of Polypropylene Microfiltration Membrane via Entrapment of an Amphiphilic Alkyl Oligoethyleneglycolether. *J. Membr. Sci.* **2010**, *349*, 312−320.
(43) Chinpa, W.; Quemener, D.; Beche, E.; Jiraratananon, R.; Deratani, A. Preparation of Poly(etherimide) Based Ultrafiltration Membrane with Low Fouling Property by Surface Modification with Poly(ethylene glycol). *J. Membr. Sci.* **2010**, *365*, 89−97.
(44) Chang, Y.; Ko, C. Y.; Shih, Y. J.; Quemener, D.; Deratani, A.; Wei, T. C.; Wang, D. M.; Lai, J. Y. Surface Grafting Control of PEGylated Poly(vinylidene fluoride) Antifouling Membrane via Surface-initiated Radical Graft Copolymerization. *J. Membr. Sci.* **2009**, *345*, 160−169.
(45) Lei, J.; Ulbricht, M. Macroinitiator-mediated Photoreactive Coating of Membrane Surfaces with Antifouling Hydrogel Layers. *J. Membr. Sci.* **2014**, *455*, 207−218.
(46) Yuan, T.; Meng, J. Q.; Hao, T. Y.; Zhang, Y. F.; Xu, M. L. Polysulfone Membranes Clicked with Poly (ethylene glycol) of High Density and Uniformity for Oil/water Emulsion Purification: Effects of Tethered Hydrogel Microstructure. *J. Membr. Sci.* **2014**, *470*, 112−124.

DOI: 10.1021/acsami.5b03625
ACS Appl. Mater. Interfaces 2015, 7, 14896−14904